View metadata, citation and similar papers at core.ac.uk
brought to you by CORE
provided by University of East Anglia digital repository

Journal of ELECTRONIC MATERIALS
DOI: 10.1007/s11664-016-4954-y
© 2016 The Author(s). This article is published with open access at Springerlink.com

Hybrid Silicon Nanostructures with Conductive Ligands and Their Microscopic Conductivity

TIEZHENG BIAN,[1] JAMIE N. PECK,[2] STEPHEN P. COTTRELL,[2] UPALI A. JAYASOORIYA,[1] and YIMIN CHAO[1,3]

1.—School of Chemistry, University of East Anglia, Norwich NR4 7TJ, UK. 2.—ISIS Facility, Rutherford Appleton Laboratory, Chilton, Didcot OX11 0QX, UK. 3.—e-mail: y.chao@uea.ac.uk

Silicon nanoparticles (SiNPs) functionalized with conjugated molecules are a promising potential pathway for generating an alternative category of thermoelectric materials. While the thermoelectric performance of materials based on phenylacetylene-capped SiNPs has been proven, their low conductivity is still a problem for their general application. A muon study of phenylacetylene-capped SiNPs was recently carried out using the HIFI spectrometer at the Rutherford Appleton Laboratory, measuring the avoided level-crossing spectra as a function of temperature. The results show a reduction in the measured line width of the resonance above room temperature, suggesting an activated behaviour for this system. This study shows that the muon study could be a powerful method for investigating microscopic conductivity of hybrid thermoelectric materials.

Key words: Silicon nanostructure, muon spectroscopy, hybrid materials, phenylacetylene, thermoelectric performance, microscopic conductivity

INTRODUCTION

Finding green energy sources and reducing greenhouse gas emissions is of paramount importance to our sustainable development. As such, developing and improving technology to enable efficient, clean energy generation is an urgent task. Thermoelectric materials generate electricity directly from temperature difference without any mechanical intervention, which makes utilizing waste heat or developing wearable charging components much easier to achieve. The efficiency of a thermoelectric material is determined by the figure of merit, ZT:[1]

$$ZT = \frac{\sigma S^2 T}{\kappa} \quad (1)$$

where σ is electrical conductivity, S is the Seebeck coefficient, κ is thermal conductivity and T is the temperature.[1]

Conjugated polymers have become attractive materials for producing thermoelectric devices.[2] Their flexibility and transparency are well suited to applications in wearable devices, along with the low working temperature range, around room temperature, rendering them superior to most traditional inorganic TE materials.[3]

Silicon is the most widely used semiconductor material. Bulk Si possesses a high Seebeck coefficient and reasonable electrical conductivity, but high thermal conductivity.[4] However, silicon nanoparticles (SiNPs) may provide a way of increasing ZT. With the structure of SiNPs, the maximization in surface area results in maximal surface defects, which in turn reduces thermal conductivity. However, this also reduces electrical conductivity. Therefore, the viability of SiNPs for use in these applications will be dependent on improving their electrical conductivity. The thermoelectric performance of phenylacetylene-functionalized SiNPs, which may be thought of as a hybrid of SiNPs and organic conductors, is proving to be a successful pathway for exploring potential TE materials.[5]

(Received June 5, 2016; accepted September 8, 2016)

Published online: 23 September 2016

Muons (μ^+, μ^- and μ^0) are radioactive decay products of the 'nuclear glue', the pions (π^+, π^- and π^0). It is the positive muon which is important in chemical applications, and it has a mean lifetime of 2.2 μs. It has a spin of ½, and has a mass approximately one ninth and magnetic moment 3.182 times that of a proton. The combination of a positive muon with an electron gives an atom called muonium (Mu), which may be considered the lightest isotope of hydrogen. Muon beams for research are produced by the bombardment of a light element target such as graphite with a beam of high-energy protons. The pions thus produced decay rapidly (lifetime ~2 ns) to give muons.[6,7]

The pions that decay to muons close to the surface of the target may be focussed into a muon beam. This positive muon is used as a probe of structure and dynamics in spectroscopy when implanted into a molecule with nearly 100% spin polarization. Muons decay to produce a positron as one of the particles, which is emitted preferentially in the direction of the spin of the muon at the time of decay. It is the latter property that makes it possible to perform spectroscopy with muons. Muon can be implanted into samples of matter in any state—solid, liquid or gaseous. After implantation, the surface muons slow rather quickly as they are thermalized, and end up in several possible states. The muon can exist, for example, as μ^+ itself, which will be a diamagnetic chemical environment, or it can capture an electron to form muonium, which would be paramagnetic. As mentioned above, the muonium has chemical properties similar to those of hydrogen atoms, and thus is extremely reactive due to the unpaired electron. Therefore, it may add to an unsaturated centre such as a multiple bond or an unsaturated ring structure to form a radical. Such radicals are known as muoniated radicals.[8] In a muon spin spectroscopy (μSR) experiment, it is the state of the muon spin that is monitored, and this reflects the local magnetic field that is felt by the muon. The local magnetic field is dominated by the unpaired electron, in the case of a radical species, and the information one obtains is a reflection of what happens to this electron. Therefore, this technique provides access to properties such as molecular/radical dynamics, reaction rates and electron transfer/conduction.

There are many variants of muon spectroscopic measurement, and the variant to be used is determined by the problem at hand. Here we report preliminary results from one of the longitudinal field muon techniques (applied magnetic field is parallel to the muon spin direction), avoided level-crossing muon spin resonance (ALC-μSR). The quantity that is measured is the forward-backward asymmetry of the muon spin in an applied field, which provides a way of measuring the level-crossing resonances that in turn provide information on the local hyperfine fields felt by the muon.[7] The technique is best explained using a simple energy diagram of a muon interacting with an electron,[9] called a Breit-Rabi diagram, illustrated in Fig. 1.

At low applied fields, there is mixing of some of the states as shown by their curving in the above diagram, but at higher fields well above that corresponding to the hyperfine field, the mixing disappears, as shown by straight line parts of the states, which are now pure Zeeman states of the system. At sufficiently high fields, the states cross each other, but if the hyperfine interaction is anisotropic, for example, one would find that these states mix with each other and thus appear to avoid each other instead of crossing. This is the so-called avoided level crossing, and the mixing of the states thus causes a loss in muon polarisation, which is measured by scanning polarisation against the applied field. The field at which this happens is given by the hyperfine interactions in the muoniated system. In muonium, there are only two spins involved, those of the muon and the electron. However, in a molecule, where

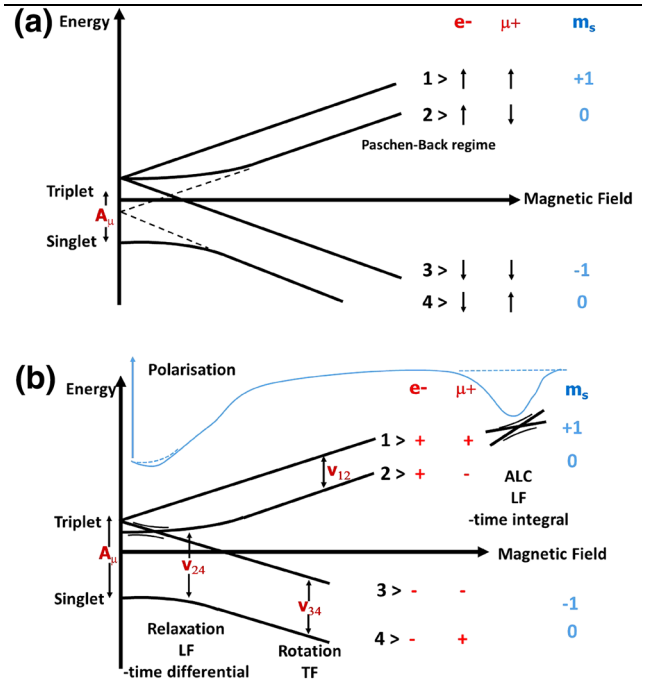

Fig. 1. The Breit-Rabi diagram: (a) Energy levels of a muon–electron system; (b) Energy levels system with a schematic representation of the transitions observed with different experimental arrangements.

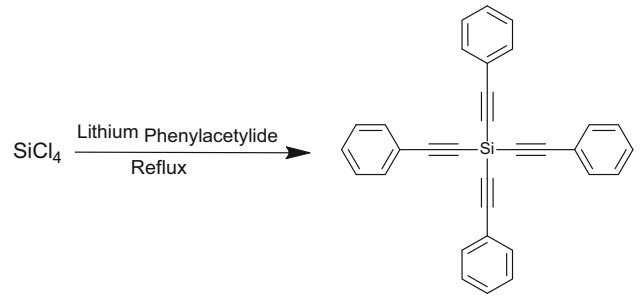

Scheme 1. Synthesis procedure of tetrakis(2-phenylethynyl)silane

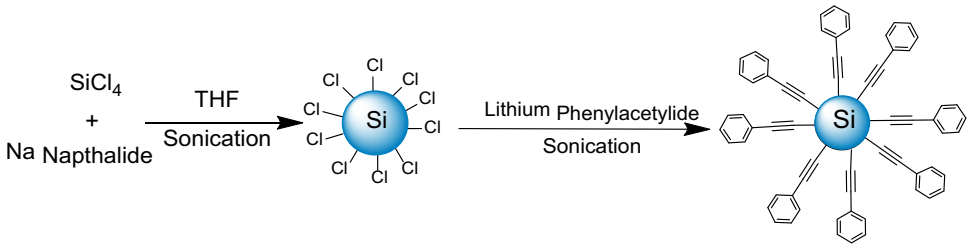

Scheme 2. Synthesis procedure for phenylacetylene-capped silicon nanoparticles.

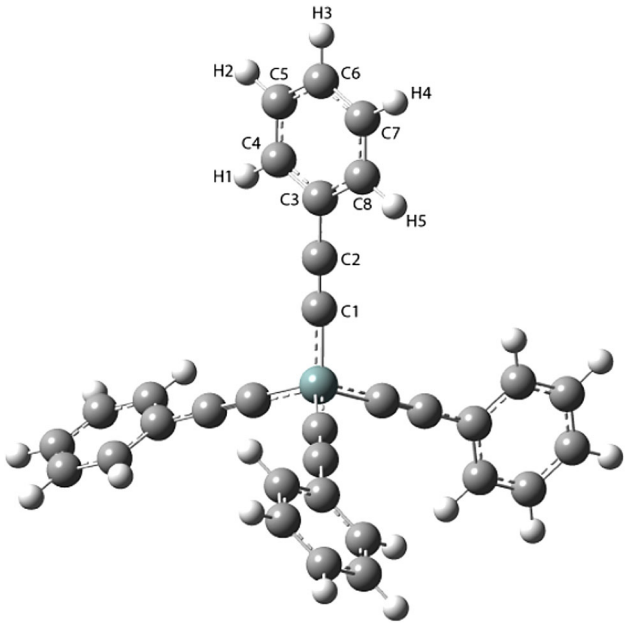

Fig. 2. 3D model of tetrakis(2-phenylethynyl)silane.

there are other atoms with nuclear spin such as H, these spins should also be mixed into the above diagram, thus resulting in more level crossings.

Based on the difference in total magnetic quantum number M, ALC resonances are sorted into three types (ΔM = 0, 1, 2). When ΔM = 0, (Δ_0 for short), the two states have the same electron spin but opposite muon and proton spins. This is also called a muon-nucleus spin flip-flop resonance. The magnetic field ($B^{\Delta 0}$) at which this resonance occurs is given by the formula below:[6]

$$B^{\Delta_0} = \frac{1}{2}\left|\frac{A_\mu - A_X}{2(\gamma_\mu - \gamma_X)} - \frac{A_\mu + A_X}{2\gamma_e}\right| \quad (2)$$

For the Δ_1 resonance, with ΔM = 1, where only the muon spin flips, the value of the external magnetic field at which this resonance occurs is given by:[6]

$$B^{\Delta_1} = \frac{1}{2}\left|\frac{A_\mu}{\gamma_\mu} - \frac{A_\mu}{\gamma_e}\right| \quad (3)$$

where A is the hyperfine coupling constant and γ is the gyromagnetic ratio, while X and μ represent nucleus and muon, respectively.[6]

Since the peak position is related to the hyperfine couplings of the muon and the proton in the radical, and the hyperfine coupling constants being characteristic of the particular muoniated radical, one could use this for assigning the observed resonances to the appropriate radical species.[10] Computer simulations of the hyperfine coupling constants are generally used to assist assignments, and the most popular such computer program is Gaussian.[11]

In this work, phenylacetylene-capped SiNPs are synthesized along with tetrakis(2-phenylethynyl)silane as the model molecule for comparison with the nanoparticles. Due to the complexity of the nanoparticle structure, it is difficult to do a computational simulation and calculation with one SiNP, and the model molecule is introduced under this circumstance. With ligands attaching to a silicon atom, it is a close imitation of the surface of the nanoparticle where the interactions occur. A computer simulation of the model molecule was performed using the Gaussian 03 software package prior to muon spectroscopic measurement, in order to guide the experiments and the data analysis.

EXPERIMENTAL PROCEDURES

A solution reduction method using sodium naphthalene was chosen to produce chloride-capped nanoparticles. This was followed by an alkylation process using lithium phenylacetylide. Similar alkylation of silicon tetrachloride molecules was performed to obtain the molecular model compound. Measurement of ALC-μSR spectra was conducted on both the molecular compound and the nanoparticle samples.

Synthesis of Tetrakis(2-Phenylethynyl)Silane

As shown in Scheme 1, a solution of phenylacetylene was mixed with n-butyllithium (n-BuLi) in tetrahydrofuran and stirred for 30 min to produce the appropriate organolithium reagent. This was then added to a dispersion of silicon chloride in tetrahydrofuran. After reflux overnight, all solvent was removed by distillation, and the residue was dissolved in toluene. After filtration, the solution was dried to produce the target compound, which was purified by recrystallization using dichloromethane, giving white needle-like microcrystals.

Table I. Calculated muon-electron hyperfine coupling constants, $A_{e\mu}$, and associated Δ_1 and Δ_0 resonance fields of the muoniated tetrakis(2-phenylethynyl)silane radical

Radical	$A_{e\mu}$ (MHz)	$\Delta_1 B_{res}$ (T)	$\Delta_0 H_1$ (T)	$\Delta_0 H_2$ (T)	$\Delta_0 H_3$ (T)	$\Delta_0 H_4$ (T)	$\Delta_0 H_5$ (T)
C_1–Mu	335.71	1.2643	1.7844	2.0118	1.7976	1.9720	1.2598
C_2–Mu	404.38	1.4495	2.3117	2.0583	2.2720	1.4433	2.2695
C_3–Mu	347.07	1.1615	1.6486	1.8172	1.1605	1.8172	1.6486
C_4–Mu	327.30	1.4565	2.2799	1.4557	2.2819	2.0685	2.3219
C_5–Mu	396.63	1.2019	1.1975	1.9202	1.6787	1.9603	1.6628
C_6–Mu	316.30	1.2745	2.0143	1.8026	2.0552	1.8026	2.0143
C_7–Mu	394.73	1.4850	2.1643	2.1665	2.1614	2.1662	2.1602
C_8–Mu	344.28	1.2328	1.8829	1.7638	1.8914	1.7639	1.8829

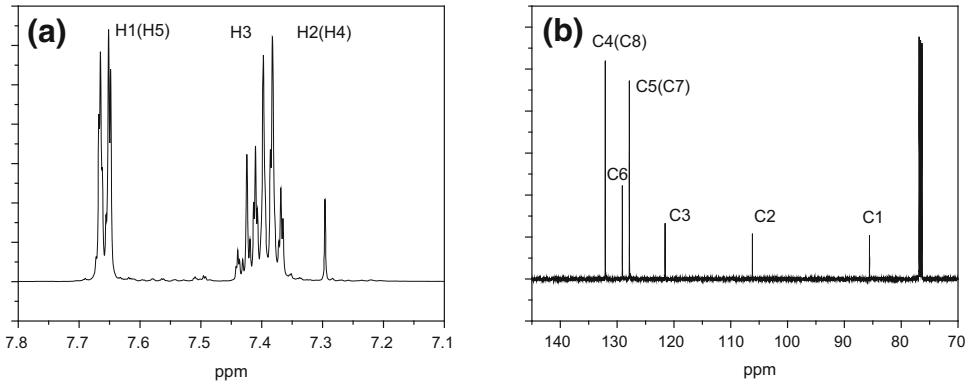

Fig. 3. Both ^{1}H-NMR (a) and ^{13}C-NMR (b) spectra prove the successful synthesis of the model molecule.

Synthesis of Phenylacetylene-Capped SiNPs

A mixture of sodium and naphthalene was sonicated for 2 h, and was then quickly added to a dispersion of silicon chloride in tetrahydrofuran. Next, an organolithium reagent made by mixing *n*-BuLi and phenylacetylene in tetrahydrofuran was added to the reaction medium, followed by overnight reflux (see Scheme 2 below). Water was then added to react with the excess lithium reagent. The organic layer was separated from the aqueous layer. All solvent was removed, and the mixture was heated under a vacuum in order to remove any residual naphthalene, giving the desired product as an orange crystalline solid powder.

ALC-μSR

The experiment was carried out using the HiFi spectrometer at the ISIS muon facility of the Rutherford Appleton Laboratory (RAL), Oxfordshire, UK. Longitudinal field scans searching for ALC resonances were performed within a field range of 1–2.8 T. This range was chosen based on the Gaussian spectral simulations. Measurements were made at various temperatures from 10 K to 380 K. Polycrystalline solid samples were mounted within aluminium sample holders sealed with Kapton windows.

^{1}H-NMR and ^{13}C-NMR

Samples were dissolved in chloroform-d. Measurements were taken with a Bruker Ascend™ 500 MHz nuclear magnetic resonance (NMR) spectrometer at room temperature.

RESULTS AND DISCUSSION

The bulk thermoelectric properties of a pellet made from phenylacetylene-capped SiNPs powder used in the present experiment were measured, as was done before, and were found to show similar results.[1] The results show the *ZT* at a value of 0.6 ± 0.1 with electrical conductivity of 18.1 ± 0.1 S m^{-1}.

In order to investigate the microscopic conductivity of phenylacetylene-capped SiNPs, tetrakis(2-phenylethynyl)silane was selected as a model molecule for comparison. Figure 2 shows a three-dimensional (3D) model of this molecule with atoms from one of the phenylacetylene labelled. Dashed lines represent the conjugated system inside this molecule, with the silicon atom at the centre. Table I is the collection of data from the ab initio density functional theory (DFT) simulations of the hyperfine parameters for this model molecule. The calculation shows all possible muon interactions within the ligand. These results identify the

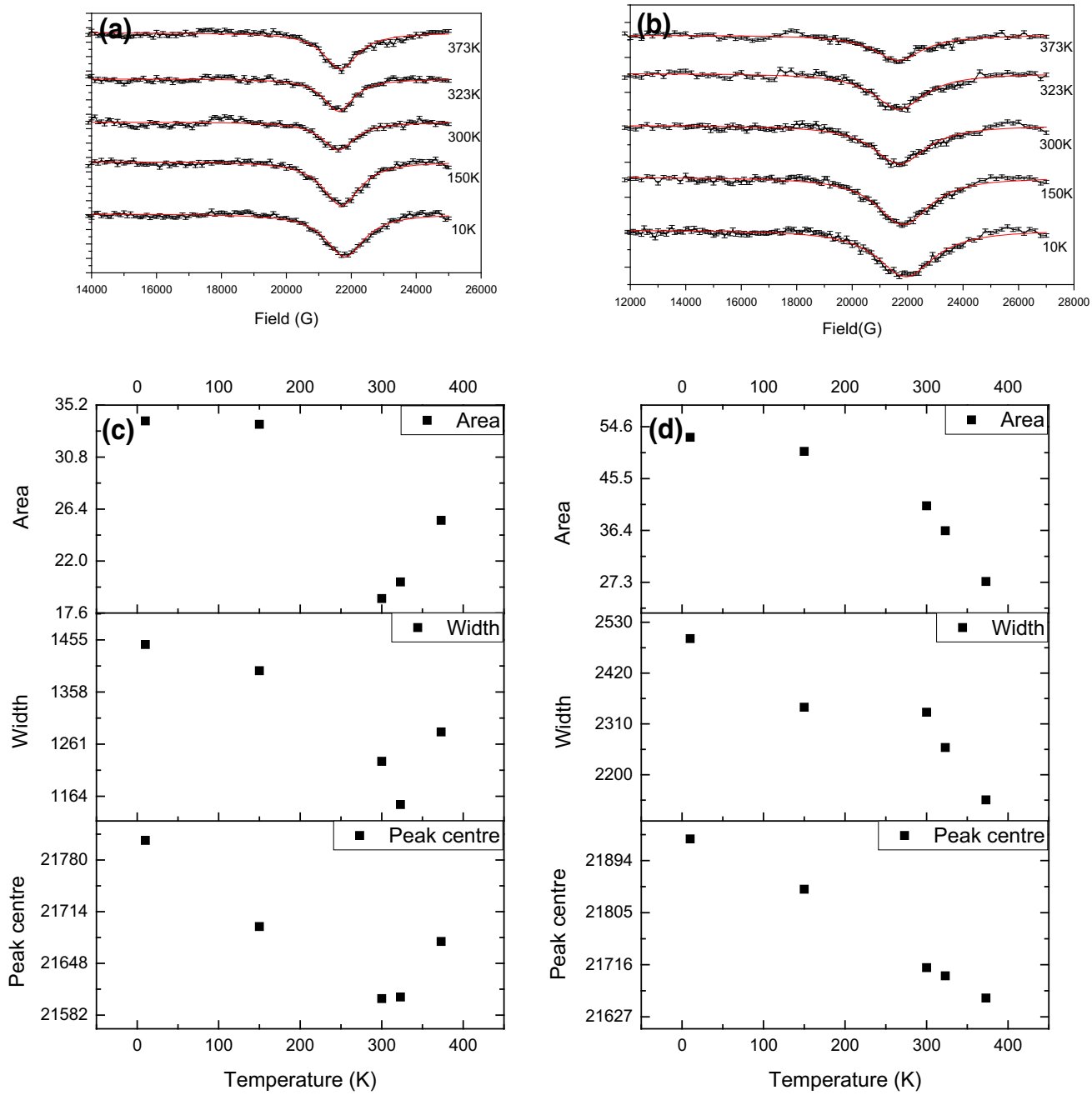

Fig. 4. ALC-μSR of tetrakis(2-phenylethynyl)silane (a) and phenylacetylene-capped SiNPs (b). Polycrystalline samples in different temperatures and corresponding integrated peak intensities, peak widths and peak positions are compared in (c) and (d).

possible positions of the external magnetic field, which in turn leads to the choice of instrument and scanning region. They also help to locate the sites to which the muons attached during the experiments.

NMR shows peaks expected from the tetrakis (2-phenylethynyl)silane molecule (see Fig. 3). Three multiplet peaks can be observed in ^{1}H-NMR at 7.66 ppm, 7.41 ppm, and 7.39 ppm, respectively; individual atoms are labelled in Fig. 3a. Six peaks are found in the ^{13}C-NMR at 132.08 ppm, 129.07 ppm, 127.84 ppm, 121.55 ppm, 106.18 ppm, and 85.59 ppm, respectively, as shown in Fig. 3b, which are consistent with carbons in six different environments within the molecule.[12] These spectra are in agreement with the previous results measured on the phenylacetylene-capped SiNPs.[1]

The ALC resonances that are observed are around 2.2 T for both the compound and the nanoparticle samples (see Fig. 4). A comparison of this with the ab initio DFT predictions (Table I) suggests an

assignment to the radical formed by the addition of muonium to the carbon C7.

In the temperature range from 300 K downwards, both the molecular sample and the nanoparticles behave in a very similar fashion, with the peak narrowing and decreasing in intensity as temperature increases. But a very distinct difference in behaviour is seen at temperatures above 300 K. The nanoparticles continue to show the same trend as at lower temperatures, while the molecular sample shows a reversal in trend, with the peak broadening and increasing in intensity with increasing temperature.

The trends that are common to both these materials may be assigned to the molecular dynamics of this ligand system, which with a reduction in temperature would gradually slow to the muon spectroscopic time window. Therefore, the distinct difference in behaviour of the nanoparticle system suggests another process entering the muon time window of measurement. We assign this to the transfer of the unpaired electron produced by the muonium addition (which may be considered as a doping process), and hence access to measurement of the microscopic electron conduction.

CONCLUSIONS

We have attempted to use muon spectroscopy to measure the microscopic electron conduction in an organic ligand-attached nanoparticle system. Preliminary results reported here show that the ALC-μSR spectroscopic technique is a uniquely promising method for studying microscopic conduction rates within organic–nanoparticle hybrid systems.

ACKNOWLEDGEMENTS

Experiments at the ISIS Pulsed Neutron and Muon Source were supported by a beam-time allocation from the Science and Technology Facilities Council.

OPEN ACCESS

This article is distributed under the terms of the Creative Commons Attribution 4.0 International License (http://creativecommons.org/licenses/by/4.0/), which permits unrestricted use, distribution, and reproduction in any medium, provided you give appropriate credit to the original author(s) and the source, provide a link to the Creative Commons license, and indicate if changes were made.

REFERENCES

1. S. Ashby, J.A. Thomas, J. Garcia-Canadas, G. Min, J. Corps, A.V. Powell, H. Xu, W. Shen, and Y. Chao, *Faraday Discuss.* 176, 349 (2014).
2. M. He, F. Qiu, and Z. Lin, *Energy Environ. Sci.* 6, 1352 (2013).
3. O. Bubnova and X. Crispin, *Energy Environ. Sci.* 5, 9345 (2012).
4. A.I. Hochbaum, R.K. Chen, R.D. Delgado, W.J. Liang, E.C. Garnett, M. Najarian, A. Majumdar, and P.D. Yang, *Nature* 451, 163 (2008).
5. S. Ashby, J. García-Cañadas, G. Min, and Y. Chao, *J. Electron. Mater.* 42, 1495 (2013).
6. I. McKenzie, *Ann. Rep. Prog. Chem. Sect. C Phys. Chem.* 109, 65 (2013).
7. C.J. Rhodes, *Ann. Rep. Prog. Chem. Sect. C Phys. Chem.* 97, 315 (2001).
8. S.L. Lee, R. Cywinski, and S. Kilcoyne, *Muon science: Muons in Physics, Chemistry and Materials*, Vol. 51 (Boca Raton: CRC Press, 1999).
9. U.A. Jayasooriya and R. Grinter, in *Encyclopaedia of Applied Spectroscopy*, ed. D.L. Andrews (Wiley-VCH, Weinheim, 2009), p. 153.
10. N.J. Clayden, *Phys. Scr.* 88, 068507 (2013).
11. J.S. Lord, *Phys. B (Amsterdam, Neth.)* 374–375, 472 (2006).
12. R. Köster, G. Seidel, I. Klopp, C. Krüger, G. Kehr, J. Süß, and B. Wrackmeyer, *Chem. Ber.* 126, 1385 (1993).